Resveratrol–Selenium Nanoparticles Alleviate Neuroinflammation and Neurotoxicity in a Rat Model of Alzheimer's Disease by Regulating Sirt1/miRNA-134/GSK3β Expression

Article *in* Biological Trace Element Research · January 2022

DOI: 10.1007/s12011-021-03073-7

CITATIONS
0

READS
71

8 authors, including:

Omayma Abozaid
Benha University. faculty of vet.med.
329 PUBLICATIONS **145** CITATIONS
SEE PROFILE

Sawsan Mohammed EL-sonbaty
Egyptian Atomic Energy Authority
106 PUBLICATIONS **339** CITATIONS
SEE PROFILE

Esraa S.A. Ahmed
Egyptian Atomic Energy Authority
7 PUBLICATIONS **36** CITATIONS
SEE PROFILE

Biological Trace Element Research
https://doi.org/10.1007/s12011-021-03073-7

Resveratrol-Selenium Nanoparticles Alleviate Neuroinflammation and Neurotoxicity in a Rat Model of Alzheimer's Disease by Regulating Sirt1/miRNA-134/GSK3β Expression

Omayma A. R. Abozaid[1] · Mohsen W. Sallam[1] · Sawsan El-Sonbaty[2] · Samy Aziza[1] · Basma Emad[3] · Esraa S. A. Ahmed[4]

Received: 12 November 2021 / Accepted: 16 December 2021

Abstract

Alzheimer's disease (AD) is a brain disorder associated with a gradual weakening in neurocognitive functions, neuroinflammation, and impaired signaling pathways. Resveratrol (RSV) has neuroprotective properties, but with low bioavailability, and low solubility in vivo. Selenium (Se) is an essential micronutrient for brain function. Thus, this study aimed to evaluate the role of formulated RSV-Se nanoparticles (RSV-SeNPs) on neurochemical and histopathological approaches associated with the AD model in rats induced by Aluminumchloride ($AlCl_3$) at a dose of 100 mg/kg/day for 60 days. RSV-SeNPs supplementation attenuates the impaired oxidative markers and mitochondrial dysfunction. The ameliorative effect of RSV-SeNPs on cholinergic deficits was associated with clearance of amyloid β (Aβ). Furthermore, activation of phosphatidylinositol 3 kinase (PI3K) deactivates glycogen synthase kinase 3 beta (GSK-3β)-mediated tau hyperphosphorylation. Additionally, RSV-SeNPs downregulate signal transducer and activator of transcription (STAT3) expression as well as interleukin-1β (IL-1β) levels, therefore alleviating neuroinflammation in AD. Moreover, RSV-SeNPs upregulate the expression of Sirtuin-1 (SIRT1) and lower that of microRNA-134, consequently increasing neurite outgrowth. Eventually, the obtained results showed that nano-formulation of resveratrol with selenium maximized the therapeutic potential of RSV against Alzheimer's disease not only by their antioxidant but also by anti-inflammatory effect improving the neurocognitive function and modulating the signaling pathways.

Keywords Aluminum, Alzheimer's disease · Resveratrol · Selenium · Neurotoxicity · Neuroinflammation · SIRT1 · miR-134

Abbreviations

Al	Aluminum
AD	Alzheimer's disease
Aβ	Amyloid β
MSCs	mesenchymal stem cells
SIRT	sirtuin
$AlCl_3$	aluminum chloride
MDA	malondialdehyde
CAT	catalase
H_2O_2	hydrogen peroxide

✉ Esraa S. A. Ahmed
esraa.tamim@yahoo.com; esraa.tamim@eaea.org.eg

Omayma A. R. Abozaid
omayma_ragab55@yahoo.com

Mohsen W. Sallam
mohsensallam55@gmail.com

Sawsan El-Sonbaty
sawsan.sonbaty@eaea.org.eg

Samy Aziza
samy.Aziza@fvtm.bu.edu.eg

Basma Emad
Basma.emad@kasralainy.edu.eg

[1] Biochemistry Department, Faculty of Veterinary Medicine, Benha University, Benha, Egypt

[2] National Center for Radiation Research and Technology, Atomic Energy Authority, Cairo, Egypt

[3] Anatomy and Embryology Department, Faculty of Medicine, Cairo University, Cairo, Egypt

[4] Radiation Biology, National Center for Radiation Research and Technology, Atomic Energy Authority, Nasr City, Cairo 11787, Egypt

Published online: 21 January 2022

GSH	glutathione
IL-1β	interleukin-1β
ANOVA	one-way analysis of variance
LSD	least significant difference
SE	standard error
STAT3	signal transducer and activator of transcription
PI3K	phosphatidylinositol 3 kinase
GSK3β	glycogen synthase kinase 3 beta
MiR-134	microRNA- 134

Introduction

Aluminum (Al) is a prevalent environmental and industrial toxin [1]. The prolonged exposure and use of the Al in daily life through inhalation, ingestion of food, drinking water, drugs, and during hemodialysis and vaccination increase its intoxications in the human body. Al causes toxicity in various organs including the liver and most importantly in the nervous system such as Alzheimer's disease (AD) [2]. AD is a neurodegenerative disorder characterized by a progressive decline of cognitive function and the loss of synapsis and neurons involved in learning and memory. In AD, the neurotoxicity and pathogenesis are mainly correlated to the extreme accumulation of misfolded proteins (hyper-phosphorylated tau protein and amyloid β (Aβ) [3, 4], oxidative stress injury, mitochondrial dysfunction, neuroinflammation, and impaired signaling pathways [5]. Aluminum chloride provokes neurotoxicity through accumulation in several areas of the brain leading to the accumulation of the most essential biomarkers for AD pathology p-tau and Aβ [6]. Moreover, its ability to cross the blood–brain barrier (BBB), impair the cholinergic neurotransmitters, induce oxidative stress and neuroinflammation along with causing brain damage and neuron apoptosis leading to synaptic plasticity abnormalities and memory loss [7].

Resveratrol (RSV) (trans-3,4,5-trihydroxystilbene) is a naturally polyphenolic phytoalexin with a stilbene structure. A large amount of RSV can be found in multiple plants, including peanuts, eucalyptus, blueberries, cranberries, and grapes [8]. Resveratrol can exhibit antioxidative, anti-inflammatory, anti-neurodegenerative, and neuroprotection via neutralizing the Aβ aggregation and its oxidative effects [9, 10]. Resveratrol interacts with numerous cellular targets, such as signaling molecules. In this way, resveratrol activates several transcription factors, inhibits several protein kinases, and downregulates the expression of inflammatory biomolecules [11].

The lower bioavailability and solubility of RSV in water minimize its therapeutic potential. Therefore, nano-formulations of RSV with Se markedly improve the bioavailability, absorption, and distribution of RSV. Moreover, nanoparticle formulation effectively protects RSV from oxidation and metabolism in animals [12]. Accordingly, the synergism between RSV and Se (an essential micronutrient for brain function has anti-inflammatory, antioxidant, and ability to attenuate the neurotoxic metals, Aβ deposition, and p-tau proteins) has a powerful neuroprotective effect [13]. Consequently, this study aims to evaluate the possible neuroprotective efficiency of resveratrol selenium nanoparticles on neurochemical and histopathological changes in a rat model of Alzheimer's disease.

Materials and Methods

Materials

Chemicals Aluminum chloride ($AlCl_3$) was purchased from El Gomhoria Company (Cairo, Egypt).

Selenium dioxide (Na_2SeO_3) and resveratrol were purchased from Sigma-Aldrich Co. All other chemicals used in the study were of analytical reagent grade.

Methods

Preparation and Characterization of RSV-SeNPs

The synthesis of RSV-SeNPs solution (10 mM) was freshly prepared in Milli-Q water. A 10 mM Na_2SeO_3 solution was prepared. First, a varied volume of 10 mM RSV solution was added dropwise into 1 mL of 10 mM Na_2SeO_3 solution, and the mixture was further diluted to10 mL with Milli-Q water. The mixed solution was heated to 70 °C. The final concentration of Na_2SeO_3 was 1.0 mM. Excess RSV and Na_2SeO_3 were removed by dialysis for 24 h [14].

The particular size and concentration of the prepared Nano is important for the biomedical application of the nanoparticles. The morphology of RSV-SeNPs was characterized by transmission electron microscopy (TEM, JEOL; model JEM2100, Japan). A sample of RSV-SeNPs was analysed through dynamic light scattering (DLS) and the particle size distribution was recorded on the ZetaSizer Nano ZS particle analyser (Malvern Instruments Limited). The surface composition and the functional groups of prepared nanoparticles were analysed using Fourier transform infrared spectroscopy (FTIR, Equinox 55 IR spectrometer). For the ultraviolet–visible absorption (UV/Vis) spectroscopy, the RSV- SeNPs sample was scanned using Shimadzu 1700 UV–Vis spectrophotometer.

Experimental Animals Thirty male Wistar rats (6–7 weeks) were purchased from the Animal Research Institute (Cairo, Egypt). Throughout the experimental period, rats were

allowed ad libitum access to food and water and housed under the same laboratory conditions with a light/dark cycle of 12 h, humidity of 50 ± 15%, and temperature of 22 ± 2 °C. All experimental procedures were performed in compliance with the standards and guidelines of the National Research Centre Ethics Committee, issued by the US National Institutes of Health, "Guide for the treatment and use of laboratory animals" for the use and protection of experimental animals (NIH publication no. 85–23, 1996).

Determination the LD_{50} of RSV-SeNPs

The determination of the LD_{50} of RSV-SeNPs administered orally was carried out on male Wistar rats according to Reed and Muench [15]. For the determination of acute lethal dose (LD_{100}) and median lethal dose (LD_{50}) of RSV-SeNPs, doses that were used were 100, 300, 500, 700, 1000, and 1500 mg/kg body weight. Mortality was recorded after 24 h, and LD_{50} was calculated as follows:

$$\text{Log LD}_{50} = \text{Log LD next below 50\%} + (\text{Log increasing factor} \times \text{proportionate distance}).$$

$$\text{Proportionate distance} = \frac{50\% - \text{mortality next below 50\%}}{\%\ \text{mortality above 50\%} - \text{mortality next below 50\%}}$$

Induction of AD and Treatments

For induction of the AD model, $AlCl_3$ was dissolved in distilled water, and the animals were given 0.5 mL of $AlCl_3$ solution at a dose of 100 mg/kg/day for 60 days [16]. Meanwhile, after induction of the AD, rats that treated with RSV-SeNPs at a dose of 200 mg/kg/day via gavage for 8 weeks.

Experimental design

After 5 days of acclimatization, the rats (100–150 g) were randomly divided into three groups ($n = 10$ per group) as follows:

I. Normal control group
II. AD group: in which rats were gavaged with $AlCl_3$
III. AD + RSV-SeNPs: in which rats were administered with $AlCl_3$ and then were treated with RSV-SeNPs

At the end of the experiment, animals were sacrificed under diethyl ether anesthesia. An incision was made on the dorsal side of the skull, and the brains were collected, cleaned, and washed with saline (0.9% sodium chloride) and stored at − 80 °C for different estimates of biochemical parameters. Some brain tissues were rinsed in 10% neutralized formalin for histopathological examination.

Biochemical Estimations

Estimation of oxidative stress markers lipid peroxidation (LPO) was assessed according to the Yoshioka et al. [17] method as malondialdehyde (MDA) levels and is recorded in the brain as µmol/g. The activity of brain catalase (CAT) was determined as H_2O_2 consumption according to the Sinha [18] method and is expressed as brain µmol/min/g. Reduced glutathione (GSH) content was measured according to the Beutler et al. [19] method and is recorded as µmol/g in the brain.

Estimation of Amyloid β and Tau Proteins Amyloid β-protein (Aβ) and phosphorylated tau protein (p-tau) concentrations were determined by rat amyloid beta-peptide 1–42 and rat phospho tau protein (PTAU) ELISA kit respectively according to the manufacture's instruction (MyBioSource Inc., San Diego, California, USA).

Determination of interleukin-1β (IL-1β) levels was estimated using the required ELISA kit according to the protocols provided by the manufacturers (RayBiotech Life, USA). Acetylcholine concentrations were determined using the fast detect acetylcholine (ACh) (rat) ELISA kit (BioVision, Inc. San Francisco, Milpitas, USA).

Western Immunoblotting

Using a TRIzol Reagent, brain tissue proteins were extracted, and protein concentrations were quantified using the *Bradford* method [20]. With 10% SDS-PAGE, 20 µg protein per lane was isolated and transferred to polyvinylidene difluoride membranes. Following 2-h incubation with Tris-buffered saline (10 mM Tris–Cl, pH 7.5, 100 mM NaCl) containing 5% nonfat-dried milk and 0.1% Tween 20, the membrane was checked as a loading control with primary antibodies to PI3K, STAT3, and GSK3β with β-actin. After washing, the membranes were washed for 2 h at room temperature with secondary monoclonal antibodies conjugated with horseradish peroxidase, and then the membranes were washed four times with the same washing buffer. Membranes were developed and visualized using the Amersham detection kit using chemiluminescence according to the manufacturer's protocols and then exposed to X-ray film. Primary

and secondary antibodies were purchased from Cell Signalling Technologies, USA. PI3K, mTOR, STAT3, and GSK3β proteins were quantified using a scanning laser densitometer by densitometric examination of the autoradiograms (Biomed Instrument Inc., USA). Results were expressed as arbitrary units after normalization for β-actin.

Molecular Investigation

Determination of mRNA gene expression of SIRT1 and MiRNA-134 by quantitative Real-Time PCR (qRT-PCR).

Real-Time PCR (qRT-PCR) in brain tissues RNA isolation and reverse transcription: The change in SIRT1 and MiRNA-134 mRNA expressions was investigated. Total RNA was isolated from 30 mg of brain tissue using the manufacturer's instructions for the TRIzol Reagent (Life Technologies, USA). Then, to validate the integrity of RNA, 1% agarose gel electrophoresis stained with ethidium bromide was used. Reverse transcriptase (Invitrogen) was used to synthesize the first strand of complementary DNA (cDNA) using 1 µg of total RNA as the manufacturer's protocol template.

Quantitative Real-Time Polymerase Chain Reaction (qPCR) In a thermal cycler step one plus (Applied Biosystems, USA), RT-PCRs were performed using the Sequence Detection software (PE Biosystems, CA). In these experiments, Table 1 lists the primer pairs used. A mixture of 25 µl total reaction volume consist of 2 × SYBR Green PCR Master Mix (Applied Biosystems), 900 nM of each prim, and 2µL of cDNA. The conditions for PCR thermal cycling included an initial step at 95 °C for 5 min, 40 cycles at 95 °C for 20 s, 60 °C for 30 s, and 72 °C for 20 s. The findings were normalized using the β-actin gene at the end of the reaction. The relative expression of the target mRNA was determined using the comparative Ct method [21].

Histopathological Analysis

In a 10% formaldehyde solution, brain tissues were fixed and were injected using conventional methods into paraffin. The section of brain tissue (3 µm) was stained with hematoxylin–eosin (H&E) stain. The stained parts were examined under a light microscope for histopathological alterations at a magnification of 400 ×.

Table 1 Sequence of the primers used for real-time PCR

Gene symbol	Primers sequence
SIRT1	F: 5′- TGTTTCCTGTGGGATACCTGA -3 R:5′-TGAAGAATGGTCTTGGGTCTTT -3′
MiRNA-134	F: 5′- GACTGGCTGTGACTGGTTGACC-3 R: 5′- GTGCAGGGTCCGAGGTATTC -3 ′
β-actin	F: 5′ CCAGGCTGGATTGCAGTT3′ R: 5′GATCACGAGGTCAGGAGATG3′

Statistical Analyses

Using one-way analysis of variance (ANOVA) followed by a post hoc test and then LeastSignificant Difference (LSD) the obtained data were expressed as the mean ± SE. The level of significance between the mean values was set at $p < 0.05$. Statistical Package for Social Science (SPSS) version 20 for Windows (SPSS® Chicago, IL, USA) software program was used to analyze the data.

Results

Characterization of RSV-SeNPs

The morphological features of RSV-SeNPs were observed on TEM (Fig. 1A). It revealed that SeNPs modified with RSV had a spherical shape. The ultraviolet–visible spectrum of RSV-selenium nanoparticles showed a surface plasmon absorption band with a maximum absorbance at 262.5 nm which can be taken as an indication for SeNPs formation (Fig. 1B). Moreover, as illustrated in Fig. 1C, the DLS analysis and zetasizer showed that the average size of the prepared RSV-SeNPs was between 60 and 90 nm. Additionally, the FTIR spectrum of RSV-SeNPs showed broadband at 3452.99 cm^{-1} representing the hydroxyl group (Fig. 1D).

Results of LD50 of RSV-SeNPs

From the results of LD_{50}, the concentration of the prepared RSV-SeNPs was found to be 200 mg/kg body weight for the oral treatment. This dose did not cause any side effects.

Effect of RSV-SeNPs on Brain Oxidative Stress Status in the AD Rat Model

$AlCl_3$ induces severe toxicity in the brain tissues leading to mitochondrial dysfunction and oxidative stress. Statistical data in Table 2 indicate a significant increase in the brain lipid peroxidation (MDA) along with a reduction in the GSH content and catalase activities in $AlCl_3$-treated group. However, treatment with RSV-SeNPs significantly reduced MDA level and improved GSH content and CAT activity respectively in the brain when compared to $AlCl_3$-treated animals.

Effect of RSV-SeNPs on Aβ-42 and Tau Proteins Concentrations in the Brain of the AD Rat Model

Changes in the levels of the most essential biomarkers for AD pathology, Aβ-42 and p-tau in the brain tissues, are

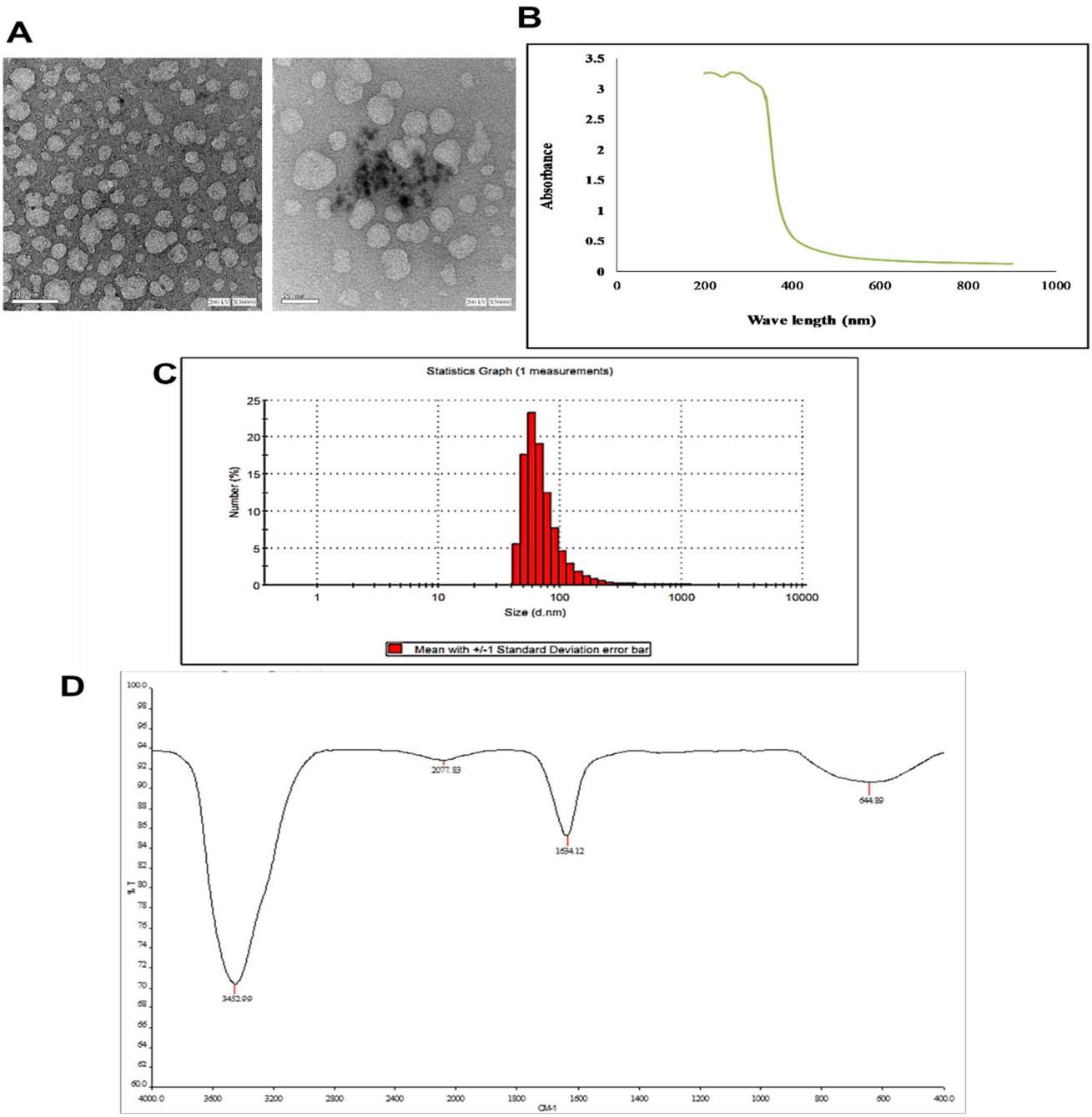

Fig. 1 **A** TEM images of RSV-SeNPs, **B** the ultraviolet–visible spectrum of RSV-SeNPs, **C** DLS analysis for size determination of RSV-SeNPs, and **D** FT-IR spectrums of RSV-SeNPs

represented in Fig. 2, which indicates that $AlCl_3$ significantly increased the levels of both Aβ-42 and p-tau in the brain tissues as compared to the control group. Alternatively, treatment with RSV-SeNPs markedly reduced the accumulation of the Aβ-42 and p-tau protein in the brain tissues of the AD rat model.

Effects of RSV-SeNPs on Neuroinflammatory Markers

Neuroinflammation results from the accumulation of Aβ-42 and p-tau in the brain tissues, causing degeneration and neuronal cell death. As shown in Fig. 3A, the levels of IL-1β

Table 2 Effect of RSV-SeNPs on brain oxidative stress status

Groups	Parameters		
	MDA ± SE (µmol/g)	GSH ± SE (µmol/g)	CAT ± S E µmol/min/g)
Control	34.8 ± 4.3^{bc}	$65.6 \pm 6.0.3^{bc}$	139 ± 5.1^{bc}
AD	110.7 ± 8.0^{ac}	23.9 ± 3.0^{ac}	70.2 ± 2.8^{ac}
AD + RSV-SeNPs	80.6 ± 5.1^{ab}	38.9 ± 3.7^{ab}	109 ± 4.5^{ab}

Values were expressed as means ± SE ($n = 6$). a, b, and c denote significant change at $p < 0.05$ versus control, AD, and RSV-SeNPs groups, respectively

in the brains of the $AlCl_3$-treated rats were significantly increased compared to the control rats. Meanwhile, treatment with RSV-SeNPs inhibits the release of IL-1β. Additionally, the Western blot data showed upregulated levels of pSTAT3 in the brain tissue of rats administered with $AlCl_3$ compared to the control group. On contrary, lower expression of pSTAT3 was detected in the RSV-SeNPs-treated group as shown in Fig. 3B. Hence, these results suggest that RSV-SeNPs suppress the inflammatory response in the brain via the inhibition of neuroinflammatory mediators.

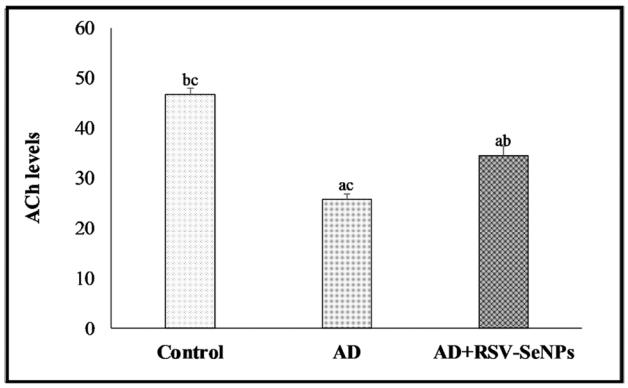

Fig. 4 Effects of RSV-SeNPs on Ach in the brain tissues. Data are presented as the means ± SE. a, b, and c denote significant change at $p < 0.05$ versus control, AD and RSV-SeNPs groups, respectively

RSV-SeNPs Treatment Improve the Cholinergic Neurotransmitter (ACh) Levels in the Brain of the AD Rat Model

Cholinergic neurotransmitters play a critical role in nearly every bodily function, ranging from muscle contraction, heart rate, gland secretion, inflammation, cognition, learning, memory, and stress response. However, impairment of the cholinergic system is implicated in AD progression. The current data revealed a statistically significant decrease in the acetylcholine (ACh) concentration in the brain tissues

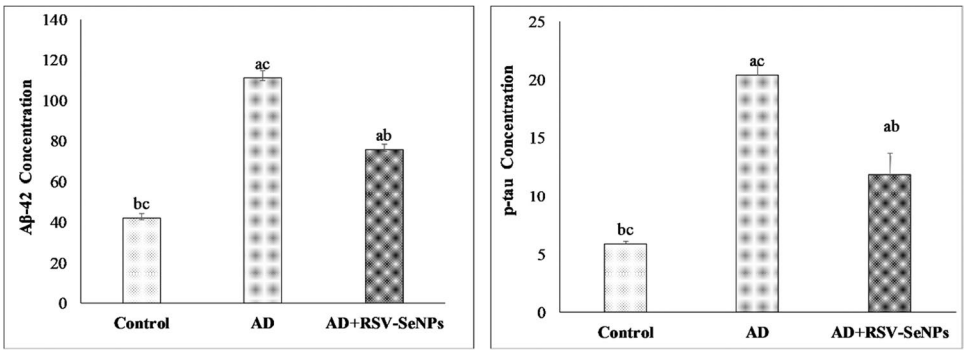

Fig. 2 Effects of RSV-SeNPs on Aβ-42 and p-tau in the brain tissues. Data are presented as the means ± SE. a, b, and c denote significant change at $p < 0.05$ versus control, AD and RSV-SeNPs groups, respectively

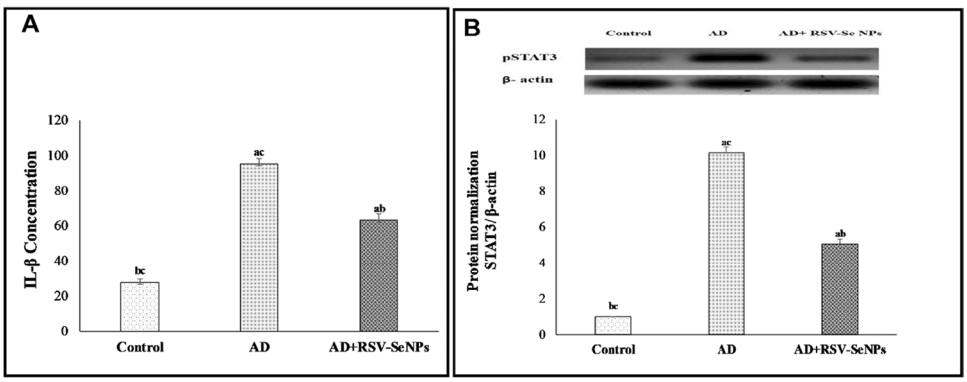

Fig. 3 Effect of RSV-SeNPs on $AlCl_3$-induced neuroinflammation, **A** IL-1β and **B** phosphorylated STAT3 in the brain tissues. Western blotting of STAT3 and β-actin (upper panel), quantitative Western blotting analysis of STAT3 and β-actin protein level (lower panel). Data are presented as the means ± SE. a, b, and c denote significant change at $p < 0.05$ versus control, AD and RSV-SeNPs groups, respectively

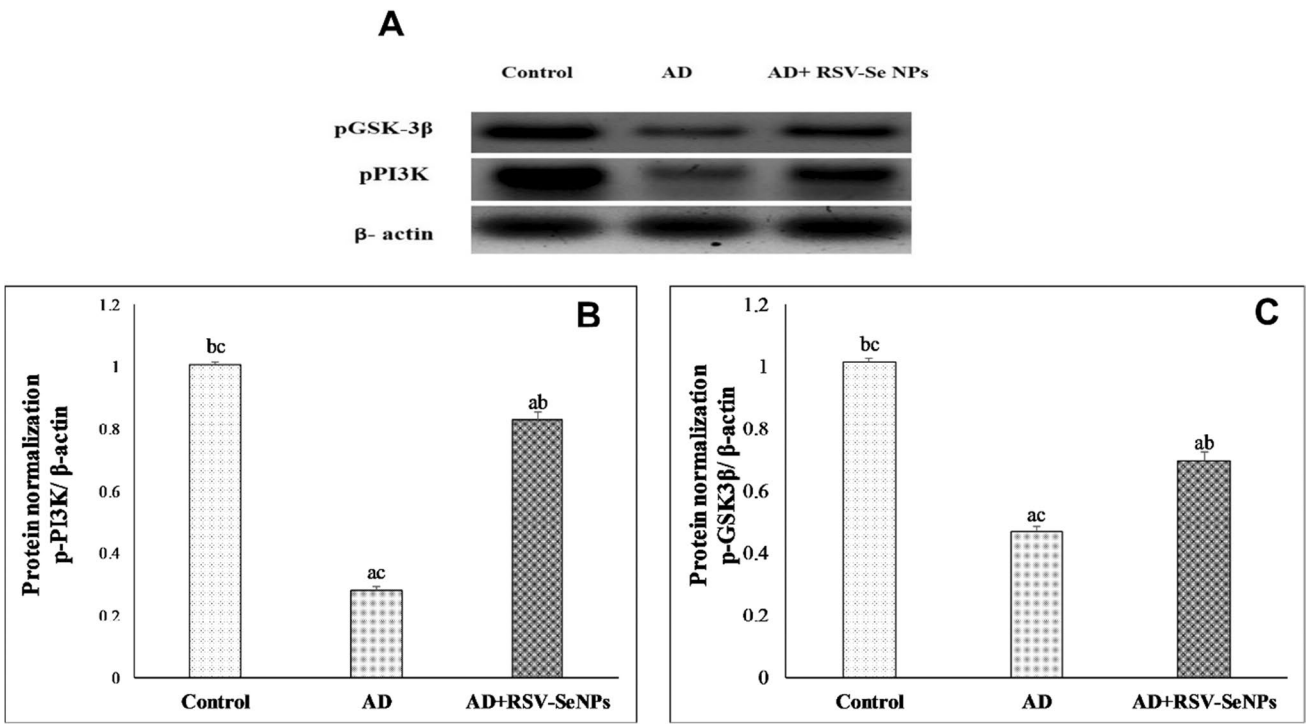

Fig. 5 RSV-SeNPs increase phosphorylation of the PI3K and GSK-3β proteins. Western blotting of PI3K, GSK-3β, and β-actin (**A**), quantitative Western blotting analysis of PI3K (**B**), GSK-3β (**C**), and β-actin protein level. Data are presented as the means ± SE. a, b, and c denote significant change at $p < 0.05$ versus control, AD and RSV-SeNPs groups, respectively

of the $AlCl_3$ group compared to the control. On the other hand, treatment with RSV-SeNPs significantly increased ACh concentration in the brain (Fig. 4).

Effects of RSV-SeNPs on the PI3K/and GSK-3β

The neurotoxic effect of Al was shown to be dependent on PI3K/and GSK-3β activity. In the present study, Western blot analysis was used to detect the expression of the p-PI3K and p-GSK-3β proteins in the brain tissues of the rats. As shown in Fig. 5, $AlCl_3$ remarkably downregulated the expression of both p-PI3K and p-GSK-3β in the brain tissues as compared to the control group. Alternatively, supplementation with RSV-SeNPs effectively upregulated p-PI3K expression as well as inhibited the activation of GSK-3β via increasing the expression of p-GSK-3β.

Effects of RSV-SeNPs on the SIRT1/MiR-134 Gene Expression

MicroRNAs (miRNAs) are important regulators of synaptic plasticity and it was found that many miRNAs are dysregulated in the human AD brain, especially miR-134 (a brain-specific miRNA). MiR-134 was shown to mediate synaptic plasticity via Sirtuin1 (SIRT1). In the current study, the gene expression of SIRT1 was significantly reduced, whereas that of MiR-134 was increased in the brain tissues of AD compared to the control group. On the other hand, treatment with RSV-SeNPs markedly reversed these results via upregulation

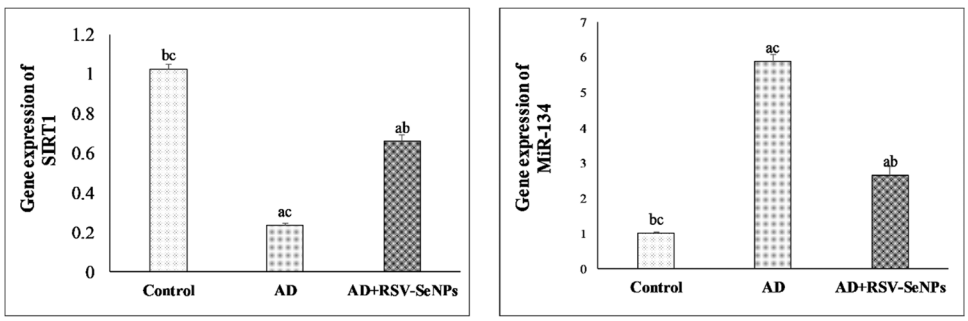

Fig. 6 Quantitative RT-PCR analysis of the mRNA level of SIRT1 and MiR-134. Data are presented as the means ± SE. a, b, and c denote significant change at $p < 0.05$ versus control, AD and RSV-SeNPs groups, respectively

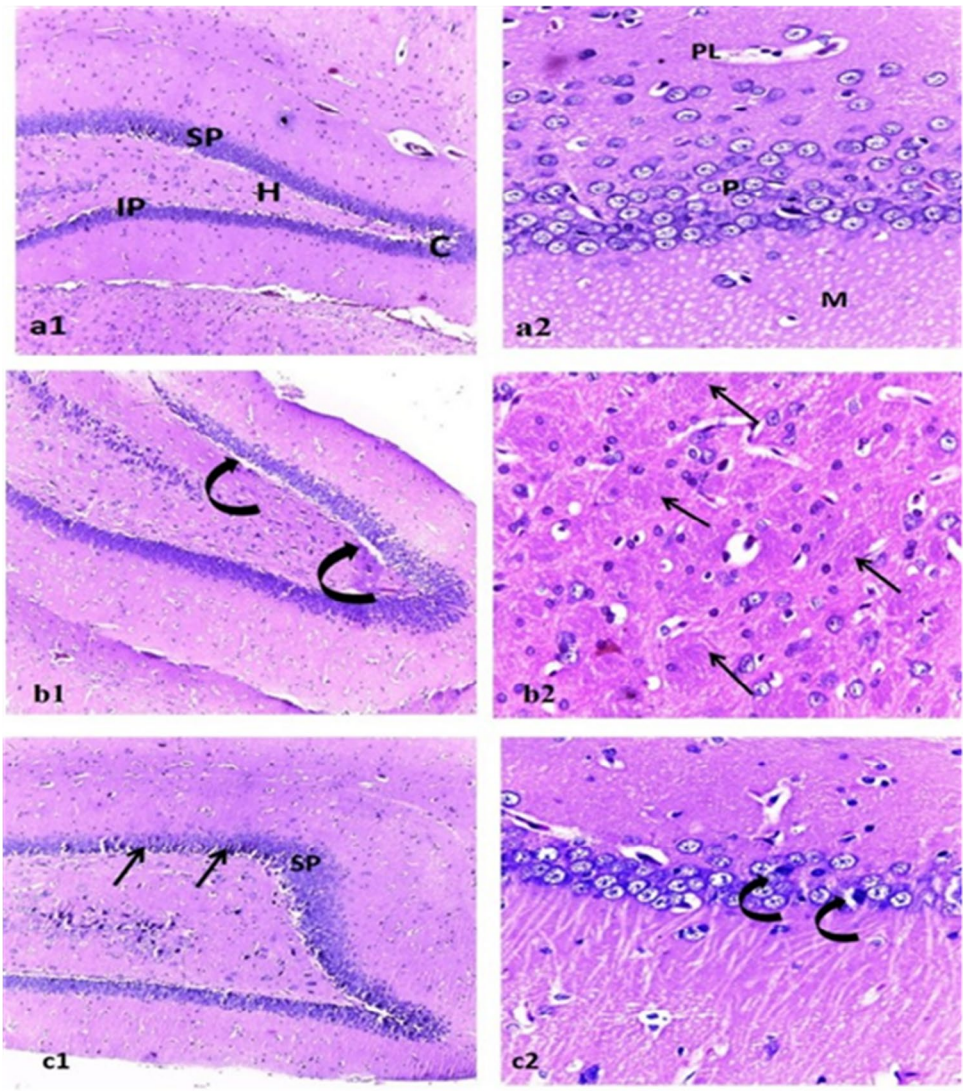

Fig. 7 Photo micrographic sections of brain tissue. Figure **a1** represents control, showing normal dentate gyrus with normal limbs (suprapyramidal (SP) and infra-pyramidal (IP)), crest (C), and hilus (H). **a2** CA1 region of the hippocampus with healthy outer polymorphic layer (PL), middle pyramidal (P), and inner molecular (M) layers. Figure **b1** represents the Alzheimer group showing dentate gyrus with vacuolations (curved arrows) invading the suprapyramidal limb. **b2** multiple cotton wool plaques (pathognomonic of Alzheimer disease) (arrows). Figure **c1** represents the RSV-SeNPs-treated group showing the increased neuronal density of the suprapyramidal (SP) limbs of the dentate gyrus with residual dark neurons (arrows). **c2** Healthy CA1 region of hippocampus except for a few shrunken pyramidal nerve cells with darkly stained cytoplasm and lost nuclear details (curved arrows). (1) H&E × 100, (2) H&E × 40

of SIRT1 and downregulation of MiR-134 gene expression (Fig. 6).

Histopathological Investigation

The photomicrograph of the brain tissue section of the control group showed a normal histological structure of the brain with normal neuronal morphology (hippocampus) (Fig. 7a1 and a2). On the other hand, the photomicrographs of brain tissue sections of the AD group showed various sizes of multiple cotton wool amyloid plaques formation in the hippocampus (Fig. 7b1). Moreover, abundant dark neurons, edema, hypoplasia, and neuronal degeneration were observed in Fig. 7b2, thus confirming the neurodegeneration within the hippocampus as compared to the control group, whereas the sections of the AD group treated with RSV-SeNPs showed an increased neuronal density in the dentate gyrus and a healthy CA1 region of the hippocampus (Fig. 7c1 and c2).

Discussion

The aluminum (Al) hypothesis is the intoxication of the brain with Al through either environmental pollution, widespread use in daily life, or medications [2]. The most affected brain regions are the hippocampus and the frontal cortex, in which Alzheimer's disease (AD) developed [22]. The neuropathology of Alzheimer's disease is associated not only with amyloid-b plaques and neurofibrillary tangles but also several impaired signal pathways due to oxidative stress injury, mitochondrial dysfunction, and inflammation [5, 23]. Therefore, the results revealed disturbances in the gene and protein expression levels of many signaling pathways involved in AD pathology, including GSK-3β and SIRT1/miRNA-134.

In harmony with the results of Fang et al. [24] and Yang et al. [25], the excessive accumulation of Aβ-42 and p-tau may be due to an imbalance in the production and clearance of β-amyloid (Aβ) peptide, together with the inability of hyper p-tau to bind with microtubules, eventually forming neurofibrillary tangles and microtubule disruption. Alternatively, in agreement with Fu et al. [26], resveratrol enhanced the clearance of neurotoxic Aβ peptides and prevented the gathering of lower molecular weight oligomers into larger plaques along with disruption of the preformed Aβ aggregates. Moreover, the RSV-SeNPs showed higher potency in the clearance of the aluminum-induced Aβ42 aggregation [12], therefore confirming the anti-amyloidogenic effect of resveratrol.

Due to higher O_2 content and polyunsaturated fatty acids along with low antioxidant levels, the brain tissues are exposed to oxidative stress and free radicals [27]. Besides Aβ accumulation, mitochondrial dysfunction causes the overproduction of ROS [28]. Consistent with Lakshmi et al. [29], the impaired redox state in the AD model was accompanied by increased brain lipid peroxidation and depletion of antioxidants, leading to neuronal damage. However, the powerful antioxidant effect of RSV-SeNPs prevents lipid peroxidation, scavenges free radicals and ROS, alleviates mitochondrial membrane disruption, and restores the levels of antioxidant enzymes [30, 31].

Besides the proteinopathy hypothesis, the cholinergic hypothesis revealed a reduction in the acetylcholine neurotransmitter in the AD brain [32]. Previous results of Ramos-Rodriguez et al. [33] reported that the accumulation of Aβ-42 and p-tau was associated with cognitive impairment due to depletion of acetylcholine. Meanwhile, RSV-SeNPs attenuated the declined levels of acetylcholine. In support of this, both Moorthi et al. [34] and Karthick et al. [35] showed that RVS improved memory loss, restored cholinergic neurotransmitters, and repaired cognitive damage through increasing brain-derived neurotrophic factor. Furthermore, Sadek et al. [36] showed that SeNPs alleviate neurotoxicity induced by cadmium via modulation of the cholinergic neurotransmitters. Consequently, nano-formulation of RSV with selenium showed a synergistic effect against aluminum-derived brain-intoxication and neurodegeneration.

Moreover, Field et al. [37] pointed out that cognitive impairments resulted from the interaction between cholinergic deficits and neuroinflammation. Prolonged activation of microglia by Aβ triggers neuroinflammatory signals and release of pro-inflammatory mediators [38, 39]. Abnormal STAT3 phosphorylation was accompanied by IL-1β secretion in Alzheimer's disease. However, inhibition of STAT3 reduced IL-1β levels and alleviated neuroinflammation [40]. Additionally, Yang et al. [25] indicate the involvement of glycogen synthase kinase-3β (GSK-3β), a downstream kinase of the PI3K/Akt signaling pathway, in neuroinflammation. The deposition of Aβ oligomers and p-tau in neurons was correlated with the inhibition of PI3K/AKT along with over-activation of GSK-3β [41, 42]. In contrast, clearance of Aβ from the brain has a neuroprotective effect via activation of the PI3K-Akt axis and downregulation of GSK-3β.

Interestingly, resveratrol inhibits inflammatory responses in the brains of rats through clearance of Aβ accumulation, lowers the production of pro-inflammatory mediators (IL-1β and STAT3), and neutralizes reactive oxygen species (ROS) [31, 43]. Furthermore, resveratrol suppresses the activation of GSK-3 β protein [44] as well as microglial cell-mediated inflammation [45].

Parallel to Yoshiyama et al. [46], SIRT1 deficiency is accompanied with higher levels of IL-1β resulting in synaptic loss and memory deficits associated with AD development. Additionally, Madadi et al. [47] reported that the dysregulation of miRNAs altered the balance between synthesis and clearance of Aβ peptide in AD. On contrary, RSV-SeNPs upregulate the expression of SIRT1 and consequently lower that of miRNA-134.

Collectively, restoring the activity of SIRT1 by RSV [48, 49] activates PI3K/Akt, which in turn downregulated the phosphorylated form GSK3β, therefore increasing neurite outgrowth, improving mitochondrial function, and reducing the production of Aβ peptides and tau phosphorylation [50, 51]. Moreover, upregulation of SIRT1 attenuates the neuroinflammatory response by suppressing the sustained activation of microglia proliferation [52]. Finally, SIRT1 directly promotes synapse plasticity and memory via a miR-134-mediated posttranscriptional mechanism. It cooperates with Yin Yang 1 (YY1) to limit the expression of miR-134 [50].

Conclusion

In conclusion, the RSV-SeNPs showed a powerful antioxidant and anti-inflammatory effect against neurotoxicity. Furthermore, RSV-SeNPs increase the clearance of misfolded proteins due to their anti-amyloidogenic potential. In addition to ameliorating both neuropathology and neurocognitive functions via improving the cholinergic deficits, RSV-SeNPs modulate various signaling pathways involved in AD pathogenesis. Overall, RSV-SeNPs could be used in the treatment of AD. However, further studies are required to determine the exact underlying mechanisms.

Data Availability All the data are available in the current study.

Declarations

Ethics Approval The experimental protocol was carried out according to the Guide for the Care and Use of Laboratory Animals (NIH no. 85–23, 1985).

Human and Animal Rights All the ethical protocols for animal treatment were followed by the National Institutes of Health Guide for the Care and Use of Laboratory Animals and supervised by the animal facilities, National Centre for Radiation Research and Technology, Atomic Energy Authority.

Conflict of Interest The authors declare no competing interests.

References

1. Igbokwe IO, Igwenagu E, Igbokwe NA (2019) Aluminium toxicosis: a review of toxic actions and effects. Interdiscip Toxicol 12(2):45–70. https://doi.org/10.2478/intox-2019-0007
2. Colomina MT, Peris-Sampedro F (2017) Aluminum and Alzheimer's disease. Adv Neurobiol 18:183–197. https://doi.org/10.1007/978-3-319-60189-2_9
3. Reitz C, Brayne C, Mayeux R (2011) Epidemiology of Alzheimer disease. Nat Rev Neurol 7(3):137–152. https://doi.org/10.1038/nrneurol.2011.2
4. Dilliott AA, Abdelhady A, Sunderland KM et al (2021) Contribution of rare variant associations to neurodegenerative disease presentation. NPJ Genom Med 6(1):80. Published 2021 Sep 28. https://doi.org/10.1038/s41525-021-00243-3
5. Lin YT, Wu YC, Sun GC, Ho CY, Wong TY, Lin CH, Chen HH, Yeh TC, Li CJ, Tseng CJ, Cheng PW (2018) Effect of resveratrol on reactive oxygen species-induced cognitive impairment in rats with angiotensin II-induced early Alzheimer's disease †. J Clin Med 7(10):329. https://doi.org/10.3390/jcm7100329
6. Liu L, Liu Y, Zhao J, Xing X, Zhang C, Meng H (2020) Neuroprotective effects of D-(-)-quinic acid on aluminum chloride-induced dementia in rats. Evid-Based Complement Alternat Med Volume, Article ID 5602597, 10 pages. https://doi.org/10.1155/2020/5602597
7. ELBini-Dhouib I, Doghri R, Ellefi A, Degrach I, Srairi-Abid N, Gati A (2021) Curcumin attenuated neurotoxicity in sporadic animal model of Alzheimer's disease. Molecules 26(10):3011. Published 2021 May 18. https://doi.org/10.3390/molecules26103011
8. Burns J, Yokota T, Ashihar H, Lean ME, Crozier A (2002) Plant foods and herbal sources of resveratrol. J Agric Food Chem 50(11):3337–3340. https://doi.org/10.1021/jf0112973
9. Malaguarnera G, Pennisi M, Bertino G, Motta M, Borzì AM, Vicari E, Bella R, Drago F, Malaguarnera M (2018) Resveratrol in patients with minimal hepatic encephalopathy. Nutrients 10(3):329. https://doi.org/10.3390/nu10030329
10. Abedini E, Khodadadi E, Zeinalzadeh E et al (2021) (2021) A comprehensive study on the antimicrobial properties of resveratrol as an alternative therapy. Evid Based Complement Alternat Med 2021:8866311. https://doi.org/10.1155/2021/8866311
11. Wang D, Li SP, Fu JS, Bai L, Guo L (2016) Resveratrol augments therapeutic efficiency of mouse bone marrow mesenchymal stem cell-based therapy in experimental autoimmune encephalomyelitis. Int J Dev Neurosci 49:60–66. https://doi.org/10.1016/j.ijdevneu.2016.01.005
12. Yang L, Wang W, Chen J, Wang N, Zheng G (2018) A comparative study of resveratrol and resveratrol-functional selenium nanoparticles: inhibiting amyloid β aggregation and reactive oxygen species formation properties. J Biomed Mater Res, Part A 106(12):3034–3041. https://doi.org/10.1002/jbm.a.36493
13. Ferro C, Florindo HF, Hélder A (2021) Santos Selenium nanoparticles for biomedical applications: from development and characterization to therapeutics. Adv Healthcare Mater 10:2100598. https://doi.org/10.1002/adhm.202100598
14. Dan L, Zuojia L, Ye Y, Yawen L (2015) Niua F (2015) Green synthesis of gallic acid-coated silver nanoparticles with high antimicrobial activity and low cytotoxicity to normal cells. Process Biochem 50(3):357–366. https://doi.org/10.1016/j.procbio.2015.01.002
15. Reed L, Muench H (1938) A simple method of estimating fifty percent end points. Am J Hyg 27:493–497
16. Justin Thenmozhi A, William Raja TR, Manivasagam T, Janakiraman U, Essa MM (2017) Hesperidin ameliorates cognitive dysfunction, oxidative stress and apoptosis against aluminium chloride induced rat model of Alzheimer's disease. Nutr Neurosci 20(6):360–368. https://doi.org/10.1080/1028415X.2016.1144846
17. Yoshioka T, Kawada K, Shimada T, Mori M (1979) Lipid peroxidation in maternal and cord blood and protective mechanism against activated-oxygen toxicity in the blood. Am J Obstet Gynecol 135(3):372–376. https://doi.org/10.1016/0002-9378(79)90708-7
18. Sinha AK (1972) Colorimetric assay of catalase. Anal Biochem 47(2):389–394. https://doi.org/10.1016/0003-2697(72)90132-7
19. Beutler E, Duron O, Kelly BM (1963) Improved method for the determination of blood glutathione. J Lab Clin Med 61:882–888
20. Bradford MM (1976) A rapid and sensitive method for the quantitation of microgram quantities of protein utilizing the principle of protein-dye binding. Anal Biochem 72:248–254. https://doi.org/10.1006/abio.1976.9999
21. Pfaffl MW (2001) A new mathematical model for relative quantification in real-time RT-PCR. Nucleic Acids Res 29(9):e45. https://doi.org/10.1093/nar/29.9.e45
22. Kot FS (2019) The effect of natural geochemical background on neurological and mental health. Exposure and Health 12:569–591
23. Hampel H, Mesulam MM, Cuello AC, Farlow MR, Giacobini E, Grossberg GT, Khachaturian AS, Vergallo A, Cavedo E, Khachaturian Snyder PJ, ZS, (2018) The cholinergic system in the pathophysiology and treatment of Alzheimer's disease. Brain 141(7):1917–1933. https://doi.org/10.1093/brain/awy132
24. Fang Y, Ou S, Wu T, Zhou L, Tang H, Jiang M, Xu J, Guo K (2020) Lycopene alleviates oxidative stress via the PI3K/Akt/Nrf-2pathway in a cell model of Alzheimer's disease. PeerJ 8:e9308. https://doi.org/10.7717/peerj.9308
25. Wen Yang, Yue Liu, Qing-Qing Xu, Yan-Fang Xian, Zhi-Xiu Lin (2020) Sulforaphene ameliorates neuroinflammation and hyperphosphorylated tau protein via regulating the PI3K/Akt/GSK-3β pathway in experimental models of Alzheimer's disease". Oxid Med Cell Longevity vol. 2020, Article ID 4754195, 17 pages. https://doi.org/10.1155/2020/4754195
26. Fu Z, Aucoin D, Ahmed M, Ziliox M, Van Nostrand WE, Smith SO (2014) Capping of aβ42 oligomers by small molecule inhibitors. Biochemistry 53(50):7893–7903. https://doi.org/10.1021/bi500910b
27. Li J, Wuliji O, Li W, Jiang ZG, Ghanbari HA (2013) Oxidative stress and neurodegenerative disorders. Int J Mol Sci 14(12):24438–24475. https://doi.org/10.3390/ijms141224438
28. Kazuki Y, Iwaharaa N, Hisaharaa S, Emotoc MC, Saitoa T, Suzukia H, Manabea T, Matsumuraa A, Matsushitaa T, Suzukia S, Kawamatad J, Sato-Akabae H, Fujiif HG, Shimohama S (2019) Transplantation of mesenchymal stem cells improves amyloid-pathology by modifying microglial function and suppressing oxidative stress. J Alzheimer's Dis 72:867–884
29. Lakshmi BV, Sudhakar M, Prakash KS (2015) Protective effect of selenium against aluminum chloride-induced Alzheimer's disease:

behavioral and biochemical alterations in rats. Biol Trace Elem Res 165(1):67–74. https://doi.org/10.1007/s12011-015-0229-3
30. Kwon KJ, Kim HJ, Shin CY, Han SH (2010) Melatonin potentiates the neuroprotective properties of resveratrol against beta-amyloid-induced neurodegeneration by modulating AMP-activated protein kinase pathways. J Clin Neurol 6(3):127–137. https://doi.org/10.3988/jcn.2010.6.3.127
31. Salehi B, Mishra AP, Nigam M, Sener B, Kilic M, Sharifi-Rad M, Fokou P, Martins N, Sharifi-Rad J (2018) Resveratrol: a double-edged sword in health benefits. Biomedicines 6(3):91. https://doi.org/10.3390/biomedicines6030091
32. Bali P, Lahiri DK, Banik A, Nehru B, Anand A (2017) Potential for stem cells therapy in Alzheimer's disease: Do neurotrophic factors play critical role? Curr Alzheimer Res 14(2):208–220. https://doi.org/10.2174/1567205013666160314145347
33. Ramos-Rodriguez JJ, Pacheco-Herrero M, Thyssen D, Murillo-Carretero MI, Berrocoso E, Spires-Jones TL, Bacskai BJ, Garcia-Alloza M (2013) Rapid β-amyloid deposition and cognitive impairment after cholinergic denervation in APP/PS1 mice. J Neuropathol Exp Neurol 72(4):272–285. https://doi.org/10.1097/NEN.0b013e318288a8dd
34. Moorthi P, Premkumar P, Priyanka R, Jayachandran KS, Anusuyadevi M (2015) Pathological changes in hippocampal neuronal circuits underlie age-associated neurodegeneration and memory loss: positive clue toward SAD. Neuroscience 301:90–105. https://doi.org/10.1016/j.neuroscience.2015.05.062
35. Karthick C, Periyasamy S, Jayachandran KS, Anusuyadevi M (2016) Intrahippocampal administration of ibotenic acid induced cholinergic dysfunction via NR2A/NR2B expression: implications of resveratrol against Alzheimer disease pathophysiology. Front Mol Neurosci 9:28. https://doi.org/10.3389/fnmol.2016.00028
36. Sadek KM, Lebda MA, Abouzed TK, Nasr SM, Shoukry M (2017) Neuro- and nephrotoxicity of subchronic cadmium chloride exposure and the potential chemoprotective effects of selenium nanoparticles. Metab Brain Dis 32(5):1659–1673. https://doi.org/10.1007/s11011-017-0053-x
37. Field RH, Gossen A, Cunningham C (2012) Prior pathology in the basal forebrain cholinergic system predisposes to inflammation-induced working memory deficits: reconciling inflammatory and cholinergic hypotheses of delirium. J Neurosci 32(18):6288–6294. https://doi.org/10.1523/JNEUROSCI.4673-11.2012
38. Kraft AD, Harry GJ (2011) Features of microglia and neuroinflammation relevant to environmental exposure and neurotoxicity. Int J Environ Res Public Health 8(7):2980–3018. https://doi.org/10.3390/ijerph8072980
39. Sarlus H, Heneka MT (2017) Microglia in Alzheimer's disease. J Clin Investig 127(9):3240–3249. https://doi.org/10.1172/JCI90606
40. Chen S, Dong Z, Cheng M, Zhao Y, Wang M, Sai N, Wang X, Liu H, Huang G, Zhang X (2017) Homocysteine exaggerates microglia activation and neuroinflammation through microglia localized STAT3 overactivation following ischemic stroke. J Neuroinflammation 14(1):187. https://doi.org/10.1186/s12974-017-0963-x
41. Chu J, Lauretti E, Praticò D (2017) Caspase-3-dependent cleavage of Akt modulates tau phosphorylation via GSK3β kinase: implications for Alzheimer's disease. Mol Psychiatry 22(7):1002–1008. https://doi.org/10.1038/mp.2016.214
42. Hyun-Jung Y (2017) Seong-Ho K (2017) The role of PI3K/AKT pathway and its therapeutic possibility in Alzheimer's disease. Hanyang Med Rev 37:18–24. https://doi.org/10.7599/hmr.2017.37.1.18
43. Ahmed T, Javed S, Javed S, Tariq A, Šamec D, Tejada S, Nabavi SF, Braidy N, Nabavi SM (2017) Resveratrol and Alzheimer's disease: mechanistic insights. Mol Neurobiol 54(4):2622–2635. https://doi.org/10.1007/s12035-016-9839-9
44. Riba A, Deres L, Sumegi B, Toth K, Szabados E, Halmosi R (2017) Cardioprotective effect of resveratrol in a postinfarction heart failure model. Oxid Med Cell Longev 2017:6819281. https://doi.org/10.1155/2017/6819281
45. Zhang F, Liu J, Shi JS (2010) Anti-inflammatory activities of resveratrol in the brain: role of resveratrol in microglial activation. Eur J Pharmacol 636(1–3):1–7. https://doi.org/10.1016/j.ejphar.2010.03.043
46. Yoshiyama Y, Higuchi M, Zhang B, Huang SM, Iwata N, Saido TC, Maeda J, Suhara T, Trojanowski JQ, Lee VM (2007) Synapse loss and microglial activation precede tangles in a P301S tauopathy mouse model. Neuron 53(3):337–351. https://doi.org/10.1016/j.neuron.2007.01.010
47. Madadi S, Schwarzenbach H, Saidijam M et al (2019) Potential microRNA-related targets in clearance pathways of amyloid-β: novel therapeutic approach for the treatment of Alzheimer's disease. Cell Biosci 9:91. https://doi.org/10.1186/s13578-019-0354-3
48. Porquet D, Griñán-Ferré C, Ferrer I, Camins A, Sanfeliu C, Del Valle J, Pallàs M (2014) Neuroprotective role of trans-resveratrol in a murine model of familial Alzheimer's disease. J Alzheimer's Dis 42(4):1209–1220. https://doi.org/10.3233/JAD-140444
49. Bastianetto S, Ménard C (1852) Quirion R (2015) Neuroprotective action of resveratrol. Biochem Biophys Acta 6:1195–1201. https://doi.org/10.1016/j.bbadis.2014.09.011
50. Cao Y, Yan Z, Zhou T, Wang G (2017) SIRT1 regulates cognitive performance and ability of learning and memory in diabetic and nondiabetic models. J Diabetes Res 2017:7121827. https://doi.org/10.1155/2017/7121827
51. Villemagne VL, Doré V, Bourgeat P, Burnham SC, Laws S, Salvado O, Masters CL, Rowe CC (2017) Aβ-amyloid and tau imaging in dementia. Semin Nucl Med 47(1):75–88. https://doi.org/10.1053/j.semnuclmed.2016.09.006
52. Cho SH, Chen JA, Sayed F, Ward ME, Gao F, Nguyen TA, Krabbe G, Sohn PD, Lo I, Minami S, Devidze N, Zhou Y, Coppola G, Gan L (2015) SIRT1 deficiency in microglia contributes to cognitive decline in aging and neurodegeneration via epigenetic regulation of IL-1β. J Neurosci 35(2):807–818. https://doi.org/10.1523/JNEUROSCI.2939-14.2015